ELSEVIER

Catalysis Today 63 (2000) 379–385

CATALYSIS TODAY

www.elsevier.com/locate/cattod

Modeling and simulation of non-isothermal catalytic packed bed membrane reactor for H_2S decomposition

P.P.Y. Chan [a], K. Vanidjee [a], A.A. Adesina [a,*], P.L. Rogers [b]

[a] *Reactor Engineering and Technology Group, School of Chemical Engineering and Industrial Chemistry, University of New South Wales, Sydney, NSW 2052, Australia*

[b] *School of Biotechnology, University of New South Wales, Sydney, NSW 2052, Australia*

Abstract

The recovery of H_2 from H_2S is an economical alternative to the Claus process in petroleum and minerals processing industries. Previous studies [React. Kinet. Catal. Lett. 62 (1997) 55; Catal. Lett. 37 (1996) 167] have demonstrated that catalytic decomposition of H_2S over bimetallic sulfide can proceed at relatively higher rates than over mono-metallic systems due to chemical synergism although conversions are still thermodynamically limited. In the present study, the performance of a catalytic membrane reactor containing a packed bed of Ru–Mo sulfide catalyst has been investigated with a view to improving H_2 yield beyond the equilibrium ceiling. A system of differential equations describing the non-isothermal reactor model has been solved to examine the effect of important hydrodynamic and transport properties on conversion. The results were obtained using a Pt-coated Nb membrane tube as the catalytic reactor enclosed in a quartz shell cylinder. Reynolds number for shell and tube side (Re^s and Re^t) as well as the modified wall Peclet number, Pe_m, dramatically affect H_2S conversions. Membrane reactor conversion rose monotonically with axial distance exceeding the equilibrium conversion by as much as eight times under some conditions.

Keywords: Claus process; Catalytic packed bed membrane reactor; H_2S decomposition

1. Introduction

Large quantities of H_2S produced during petroleum hydrotreatment operations and metal ore reduction processes are often removed from industrial gaseous effluent via the Claus reaction or absorption into alkanolamines. Although re-salable sulfur may be obtained, these H_2S removal options convert useful H_2 into non-profitable low grade water. The catalytic decomposition of H_2S to hydrogen and sulfur, both of which are highly valuable, offer the possibility for improving overall plant economics [3].

Several investigators have examined the catalytic splitting of H_2S over transition metal sulfides. Evidence suggests that bimetallic Mo-containing sulfides exhibit some of the best activities [1,2]. However, since the reaction is reversible and strongly endothermic ($\Delta H_{298} = 85.2\,\mathrm{kJ/mol}$), conversion and H_2 yield are limited by thermodynamics. It is therefore expected that a system in which simultaneous product H_2 separation from the reaction can take place will improve process performance. A catalytic packed bed membrane reactor immediately suggests itself.

Buxbaum and Kinney [4] have presented H_2 permeation data for several metals as a function of temperature. Since catalytic H_2S decomposition proceeds only at reasonable rates from about 873 K, the reactor would be fabricated from metallic membranes that

* Corresponding author. Tel.: +61-2-9385-5268; fax: +61-2-9385-5966.
E-mail address: a.adesina@unsw.edu.au (A.A. Adesina).

0920-5861/00/$ – see front matter
PII: S0920-5861(00)00482-X

Nomenclature

A	reactor cross-sectional area
C_p	heat capacity of gas
d	thickness of membrane
F	volumetric flow rate
h	overall heat transfer coefficient
ΔH	heat of the H_2S decomposition reaction
J	flux across the membrane
k	reaction rate constant
K_{eq}	equilibrium constant for H_2S decomposition reaction
L	reactor length
M	molecular weight
P	partial pressure
$\mathcal{P}$	permeability
Pe_m	modified Peclet number
r_{H_2S}	rate of reaction
Re	Reynolds number
S	surface area per unit length
T	temperature
z	dimensionless reactor length coordinate

Greek letter

μ	viscosity of gas

Subscript

Ar	argon gas
H_2	hydrogen gas
H_2S	hydrogen sulfide gas
M	membrane
mix	gas mixture
tot	total
i	component i

Superscripts

f	furnace
in	inlet
s	shell side
t	tube side

show excellent permeation coefficient and H_2 permselectivity at this elevated temperature. Among others, niobium offers an excellent H_2 permeation rate in the range 700–1100 K. To avoid H_2S corrosion at these temperatures, Nb tube would be internally coated with platinum which also enjoys comparable H_2 permeability. Thus the packed bed reactor consisted of a composite Nb/Pt membrane encased in a quartz cylinder (shell). The annular space between the Nb/Pt tube and the quartz shell is swept by an inert gas to carry away the permeated H_2. The membrane tube is packed with a Ru–Mo sulfide since the kinetic expression for H_2S decomposition over this catalyst has been previously obtained [2].

In view of the endothermic nature of the reaction, the catalytic packed bed membrane reactor (CPBMR) is deemed to operate non-isothermally. The present work is therefore focused on a parametric study of the reactor system to provide a basis for experimental optimization.

2. Model development

A schematic diagram of the shell-and-tube membrane reactor is shown in Fig. 1. The sweep gas through the shell (annulus) side is pure (inert) argon while the feed is an H_2S/argon mixture. Both streams are preheated to at least 873 K before entering the reactor system which is itself placed in a temperature-controlled furnace. For the purpose of model development, it is assumed that:

1. plug flow conditions exist in both shell and tube sides;
2. negligible axial pressure drop prevails in both packed bed and annular space;
3. constant sweep gas flow rate since permeated H_2 flow rate is relatively low;
4. H_2 permeation through the Nb/Pt membrane follows Sievert's law [5], thus, cross-flow H_2 flux, J_{H_2}, is

   $$J_{H_2} = U[(P^{t}_{H_2})^{1/2} - (P^{s}_{H_2})^{1/2}] \quad (1)$$

   where the overall permeation coefficient, U, is related to H_2 permeability through Pt and Nb as

   $$\frac{1}{U} = \frac{d^{m}_{Pt}}{\mathcal{P}_{Pt}} + \frac{d^{m}_{Nb}}{\mathcal{P}_{Nb}} \quad (2)$$

   Neither H_2S nor S_2 molecules permeate through to the shell side, i.e. 100% H_2 permselectivity;
5. membrane is catalytically inactive;
6. reactant and sweep gas flow co-currently.

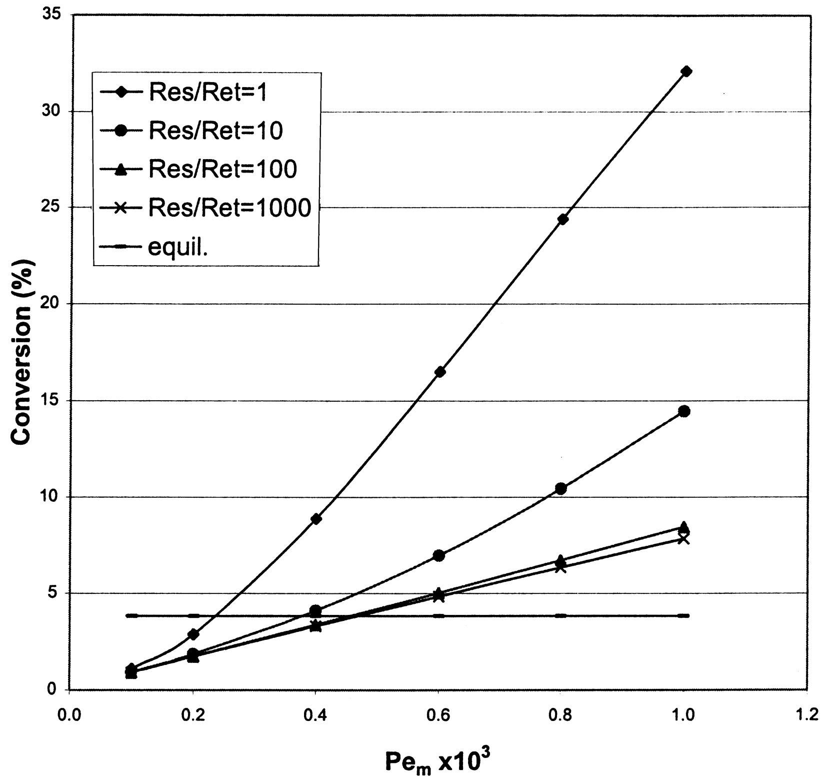

Fig. 1. H_2S conversion against Pe_m for Re^s/Re^t ratio of 1, 10, 100, and 1000 at the inlet temperature of 873 K.

Based on these assumptions, the steady-state mass and energy balances may be written as follows:

Tube side balances:

$$\frac{dP^t_{H_2S}}{dz} = -\left[\frac{(P^t_{tot})^{1/2} Pe_m d^t}{4U}\right](-r^t_{H_2S}) \tag{3}$$

$$\frac{dP^t_{H_2}}{dz} = \left[\frac{(P^t_{tot})^{1/2} Pe_m d^t}{4U}\right]\left[(-r^t_{H_2S}) - J_{H_2}\frac{S^t}{A^t}\right] \tag{4}$$

$$\frac{dT^t}{dz} = \left[\frac{Pe_m}{U(P^t_{tot})^{1/2}\pi d^t C_{p\,mix}^{\,t}}\right] \times \left[(-\Delta H)(-r_{H_2S})A^t - S^t(T^t - T^s) \times \left(J_{H_2} C_{pH_2} + \frac{h}{2}\right)\right] \tag{5}$$

Shell side balances:

$$\frac{dP^s_{H_2}}{dz} = \left[\frac{P^s_{tot} Pe_m Re^t d^t M_{mix}\mu_{mix}}{(P^t_{tot})^{1/2} Re^s d^s M_{Ar}\mu_{Ar}}\right] J_{H_2} \tag{6}$$

$$\frac{dT^s}{dz} = \left[\frac{Pe_m Re^t M_{mix}\mu_{mix}}{Re^s M_{Ar}\mu_{Ar} U (P^t_{tot})^{1/2}\pi d^s C_{p\,mix}^{\,s}}\right] \times \left[S^t(T^t - T^s)\left[J_{H_2} C_{pH_2} + \frac{h}{2}\right] + h^f S^s(T^f - T^s)\right] \tag{7}$$

with the boundary conditions at

$$z = 0,\ P^t_{H_2S} = P^{in}_{H_2S},\ P^t_{H_2} = 0,\ P^s_{H_2} = 0,\quad T^t = T^{in},\ \ T^s = T^{in} \tag{8}$$

where

$$Re^t = \frac{4F^t_{tot}}{\pi M_{mix} d^t \mu_{Ar}},\qquad Re^s = \frac{4F^s_{tot}}{\pi M_{Ar} d^s \mu_{Ar}} \tag{9}$$

$$Pe_m = \frac{U(P^t_{tot})^{1/2} d^t L\pi}{F^t_{tot}} \tag{10}$$

Table 1
Heat of reaction and gas heat capacity parameters $\Delta H_{298} = 85.2\,\mathrm{kJ/mol}$

Component	ν	α	β	γ
H_2S	-1	7.2	3.6×10^{-3}	0
S_2	0.5	8.58	3×10^{-4}	0
H_2	1	6.62	8.1×10^{-4}	0

$$-r_{H_2S} = k_{H_2S} P_{H_2S} - \frac{1}{K_{eq}} (P_{H_2})^{1/2} \tag{11}$$

$$\ln K_{eq} = \frac{10215.2}{T} - 2.44 \ln T \tag{12}$$

$$\Delta H = \Delta H_{298} + \int_{298}^{T} \Delta C_p \, dT \tag{13}$$

$$\Delta C_p = \sum \nu_i C_{pi} \tag{14}$$

$$C_p = \alpha + \beta T^t + \gamma (T^t)^2 \tag{15}$$

Values of ΔH_{298}, ν, α, β, and γ are presented in Table 1.

Table 2
Membrane reactor data and operating conditions

Parameter	Values
Length of catalytic bed	0.6 m
Diameter of reactor tube	9.017×10^{-3} m
Diameter of reactor shell	1.96×10^{-2} m
Thickness of platinum film	5×10^{-6} m
Thickness of niobium membrane	3×10^{-3} m
Pressure of reaction gas	101.325 kPa
Pressure of sweep gas	50.663 kPa
Furnace input temperature	1173 K
k_{H_2S}	$7.11 \times 10^2\, e^{-92\,106/RT^t}$ mol (gcat)$^{-1}$ s^{-1} kPa^{-1}

3. Results and discussion

The system of ordinary differential equations (Eqs. (3)–(8)) was solved using a fourth order Runge–Kutta method. It is, however, easily seen that the solution behavior will be a function of the fluid dynamics (Re^s, Re^t), membrane characteristics namely, cross-flow modified Peclet number, Pe_m, and inlet

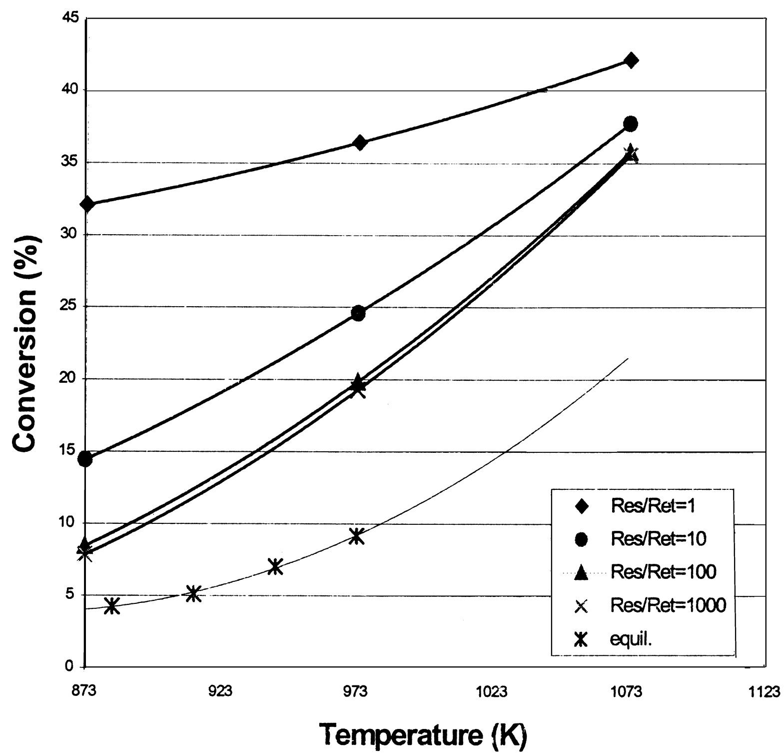

Fig. 2. Effect of temperature on H_2S conversion for Re^s/Re^t ratio of 1, 10, 100, and 1000 with $Pe_m = 1 \times 10^{-3}$.

temperature, T^{in} (both shell and tube sides). Consequently, the numerical results will be interpreted in terms of Re^s/Re^t ratio, Pe_m and T^{in}.

Table 2 provides a summary of the reactor specifications. Preliminary sensitivity analysis reveals that feasible solutions are only possible for $10^{-5} \leq Pe_m \leq 10^{-3}$ and $Re^s/Re^t \geq 1$.

Inlet temperature T^{in} was varied between 873 and 1073 K since catalytic rates are compounded by H_2S thermolysis at about 1043 K.

Fig. 1 shows that H_2S conversion increased monotonically with Pe_m. However, the effect was more pronounced at low Re^s/Re^t ratio with predicted reactor conversion of about eight times that at equilibrium (4%) at $Pe_m = 10^{-3}$. The increase in H_2S conversion with Pe_m is probably due to an increase in H_2 flux across the membrane and thus reduced H_2 partial pressure in the packed bed. In accordance with Le Chatelier's principle, H_2S decomposition in the packed bed would be shifted towards the right.

The relatively poor conversions recorded at $Re^s/Re^t > 1$ is indicative of low transmembrane H_2 flux at high sweep gas flow rates. A similar observation was made in the study of methane reforming in Pd membrane reactor [6]. As may be seen from Fig. 1, optimum H_2S conversion was obtained at $Re^s/Re^t = 1$. The effect of inlet temperature on H_2S conversion is illustrated in Fig. 2. It is apparent that conversion increased with temperature consistent with the endothermic nature of the reversible reaction. Interestingly, under all flow conditions investigated, the membrane reactor gave better conversions than thermodynamic equilibrium values.

Axial conversion profiles within the inner packed bed are shown in Fig. 3(i). The horizontal solid line corresponds to the equilibrium conversion at the inlet reactor condition. It is significant that conversion values are better almost anywhere in the reactor for $Re^s/Re^t = 1$. In particular conversion in excess of equilibrium were attained much earlier in the reactor than under the flow conditions in these plots. Fig. 3(ii) shows the influence of hydrodynamics and membrane properties on the H_2 removal ratio, defined as the ratio of the H_2 molar flow rate in the shell side to the H_2 production rate in the tube side. Low Re^s/Re^t values favor the H_2 removal ratio at a given modified Peclet number, Pe_m. However, when the latter is decreased by say two orders of magnitude even at Re^s/Re^t, the H_2 removal ratio substantially drops as may be seen by comparing curve a with d. Although not shown, the removal ratio does not change with inlet or reaction temperature.

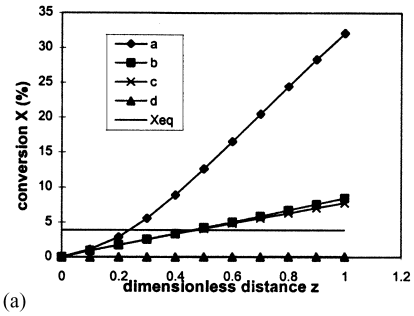

(a)

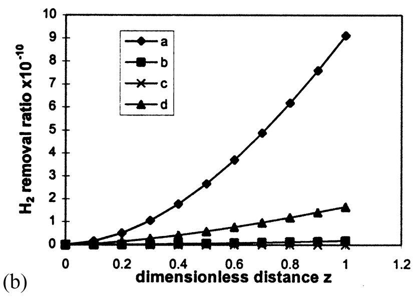

(b)

Fig. 3. (i) Axial conversion and (ii) H_2 removal ratio profile. a: $Pe_m = 10^{-3}$, $Re^s/Re^t = 1$; b: $Pe_m = 10^{-3}$, $Re^s/Re^t = 100$; c: $Pe_m = 10^{-3}$, $Re^s/Re^t = 10\,000$; d: $Pe_m = 10^{-5}$, $Re^s/Re^t = 1$.

Fig. 4 plots the temperature profile within the reactor. Inlet temperature appears to be a determinant of the axial temperature distribution at the lowest temperature studied (873 K). Temperature on both shell and tube sides rose monotonically from the inlet value before leveling off about half-way through the reactor to a plateau. However, the shell side temperature, T^s was always higher than the tube temperature, T^t, since the shell is directly in contact with the furnace wall maintained at 1173 K. There is, however a large temperature difference (100 K) between the quartz surface and the membrane wall. As the inlet temperature increased, the reaction side temperature, T^t, initially dropped before rising almost linearly to a

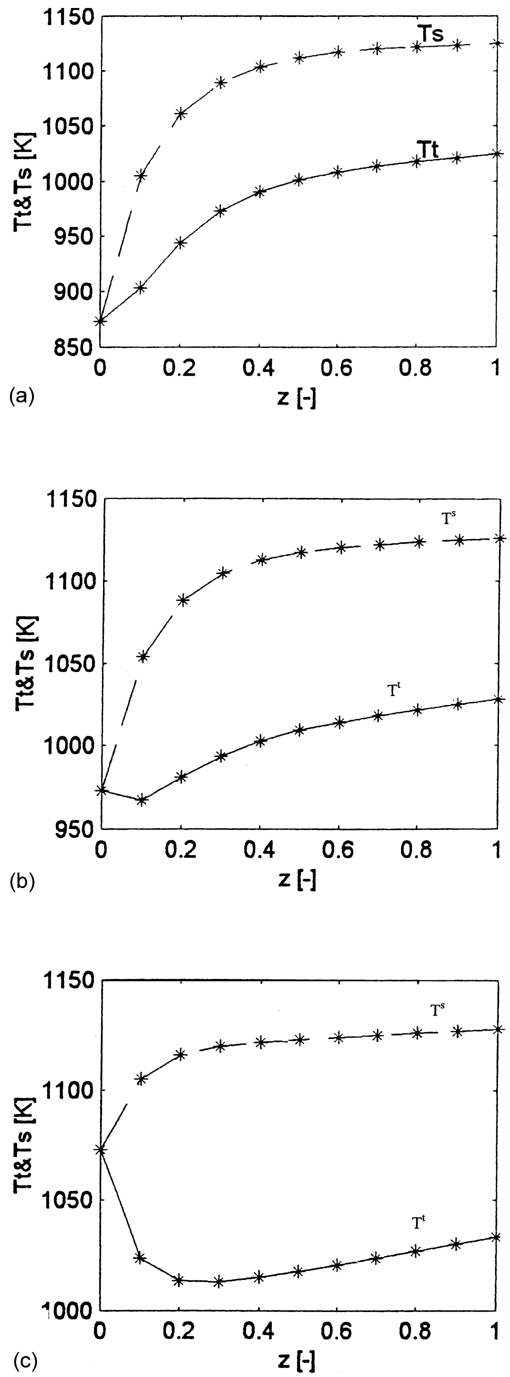

Fig. 4. (a) Temperature profile within the reactor for $Re^s/Re^t = 1$, $Pe_m = 1 \times 10^{-3}$, and inlet temperature at 873 K, (b) Temperature profile within the reactor $Re^s/Re^t = 1$, $Pe_m = 1 \times 10^{-3}$, and inlet temperature at 973 K, (c) Temperature profile within the reactor $Re^s/Re^t = 1$, $Pe_m = 1 \times 10^{-3}$, and inlet temperature at 1073 K.

higher exit temperature. The pattern is expected in an externally heated endothermic reactor operation and a similar behavior is also registered for $T^{in} = 1073$ K. T^s profile in the shell side however was unchanged at all three inlet temperature levels probably because the temperature distribution is entirely governed by convective thermal transport since no reaction occurs within the annular space. Better conversions at low Re^s/Re^t ratio is evidence of better heat transfer to the membrane wall and hence the packed bed as a result of longer fluid residence time in the shell side.

4. Conclusion

This work has demonstrated that catalytic H_2S decomposition may offer higher than equilibrium conversion when carried out in an appropriate membrane reactor. Parametric studies based on steady-state non-isothermal model of the double pipe tubular reactor indicate that up to 8-fold increase in conversion (beyond thermodynamic limitation) may be obtained at low ratio of shell side Reynolds number to tube side Reynolds number. Conversion and hence H_2 yield also improved with higher transmembrane modified Peclet number, although this value is bounded between 10^{-5} and 10^{-3}. Thus for a given membrane, material variation in Pe_m may be advanced by decreasing membrane thickness to improve overall H_2 permeation coefficient.

Acknowledgements

The authors are grateful to the Australian Research Council for financial support.

References

[1] M. Gwaunza, A.A. Adesina, The performance of a Ru–Mo sulfide catalyst for H_2S decomposition, React. Kinet. Catal. Lett. 62 (1997) 55.

[2] S.C. Moffat, A.A. Adesina, The dissociation kinetics of H_2S over an alumina supported Co–Mo sulphide catalyst, Catal. Lett. 37 (1996) 167.

[3] M.E.D. Raymont, Hydrogen: production and marketing, ACS Symp. Ser. 116 (1980) 333.

[4] R.E. Buxbaum, A.B. Kinney, Hydrogen transport through tubular membranes of palladium-coated tantalum and niobium, Ind. Eng. Chem. Res. 35 (1996) 530.
[5] S.A. Steward, Review of hydrogen isotope permeability through materials, Lawrence Livermore National Laboratory, California, 1983.
[6] E. Kikuchi, Hydrogen — permselective membrane reactors, Cattech (March 1997) 67.